Sensitivity of the present INTOR layout to variations of some performance objectives

K. Borrass

IPP 2/257

May 1982

MAX-PLANCK-INSTITUT FÜR PLASMAPHYSIK

8046 GARCHING BEI MÜNCHEN

MAX-PLANCK-INSTITUT FÜR PLASMAPHYSIK

GARCHING BEI MÜNCHEN

Sensitivity of the present INTOR layout to variations of some performance objectives

K. Borrass

IPP 2/257 May 1982

Die nachstehende Arbeit wurde im Rahmen des Vertrages zwischen dem Max-Planck-Institut für Plasmaphysik und der Europäischen Atomgemeinschaft über die Zusammenarbeit auf dem Gebiete der Plasmaphysik durchgeführt.

IPP 2/257 K. Borrass

Sensitivity of the present INTOR layout to variations of some performance objectives

May 1982 (in English)

Abstract

The sensitivity of the INTOR layout to variations of the main performance objectives and design specifications is studied with the SUPERCOIL layout model. The stored energy (E_m) and the outer coil radius (R_2) are used as figures of merit. The objectives and specifications under consideration are the neutron wall load, the neutron fluence, the ignition margin and the blanket modularity respectively.

Sensitivity of the present INTOR layout to variations of some performance objectives

K. Borrass

1. Introduction

The sensitivity of the present INTOR layout to variations of the performance parameters N_n^m (minimum neutron wall load), C^m (minimum ignition margin), W_{int}^m (minimum neutron fluence), and ε^m (maximum field ripple) is studied. In addition, the effect of a higher blanket modularity is considered.

Calculations are performed with the SUPERCOIL layout program, a brief description of which was given in Ref. /1/. The main components involved in SUPERCOIL are the plasma, the TF system, and the OH transformer. Emphasis is placed on taking into account physical and technical limitations as well as constraints that result from imposing performance objectives. Among the solutions that meet all constraints that which optimizes a prescribed figure of merit is selected. For the calculations presented here the energy stored in the TF system is taken as figure of merit. This choice, which is mainly determined by the lack of a cost model, is, however, of minor importance for the comparative studies intended in this study. Furthermore, the optimization is insensitive to this approximation as long as the cost of the system depends monotonically on the respective figure of merit.

It is pointed out that no prescription is made as to whether a constraint is met or not (in general not all constraints can be met simultaneously), but this information is part of the result.

We proceed in the usual way. First a reference case is established. Then the variation of single quantities is studied, the other parameters of the reference case being kept fixed. Finally, benchmark calculations combining variations of different performance objectives are made.

2. Reference case

The Phase I version of INTOR is taken as reference case. At first consistency between the present INTOR layout and the SUPERCOIL model has to be demonstrated. This is done by taking the present INTOR data as input for the code as illustrated by Table 1. The input data consist of two groups. The first group comprises limit values characterizing the respective constraint. The second group comprises quantities which cannot be chosen freely (such as the safety factor q(a)) or have only slight impact on the system (such as the scrape-off layer thickness l). All other quantities are self-consistently determined. For those quantities for which no reference value was available reasonable estimates were made. This mainly concerns the coil layout.

The ignition margin was evaluated for the present INTOR layout on the bais of the model involved in SUPERCOIL. The resulting value is then taken as input. It must be noted that the ignition margin is not normalized to unity for marginal ignition. A value $C \simeq 1.3$ corresponds to marginal ignition if favourable profiles and a clean plasma are assumed.

The reference neutron wall load was determined by an analogous procedure resulting in a value of 1.82 MW/m^2 instead of 1.3 MW/m^2. The discrepancy is partly due to a more optimistic estimation of the useful beta ($\bar{\beta}_t$ = 0.12 s/A) and partly due to a more optimistic estimation of the fusion power density (p_f [MW/m^3] = 2.0 $\bar{\beta}_t^2$ B_t^{o4} [T]), which was chosen on the basis of 1-D simulations. To rescale to the INTOR assumptions, quantities which are proportional to p_f have to be divided by 1.4.

In all calculations the TF coils use Nb_3Sn, while the OH coils use NbTi as superconducting material. Copper is used as stabilizer throughout.

Figure 2 illustrates the way in which the maintenance condition is taken into account. A segmentation which is I_d times N is simulated by imposing the constraint

$$\frac{2\pi\,(R_o + a + u + 1)}{N\,I_d} + \frac{0.6}{I_d} + 0.2 \leq d^* \,, \quad (1)$$

where $I_d = 1, 2, \ldots$. (For explanation of the symbols see Tables 1 and 2.) The second and third terms on the left-hand side of eq. (1) are chosen such that the INTOR reference data are well reproduced for $I_d = 1$.

In Table 2 the main output data as given by SUPERCOIL are listed. Obviously, the INTOR data are well reproduced.

3. Trade-off studies

3.1 Variation of the blanket segmentation

A blanket segmentation which is I_d times N is treated by taking the appropriate value for I_d in the constraint described by eq. (1). When I_d is increased over unity, with all other input data kept fixed to their reference values, essentially no effect is observed, contrary to the expected reduction of R_2.

In the reference case R_2 is determined by eq. (1). As one concludes from Table 2, the ripple constraint is, however, nearly met in this case. If now condition eq. (1) is relaxed by taking $I_d > 1$, the ripple condition becomes effective and prevents R_2 from decreasing. The ripple condition thus has to be relaxed to benefit from higher modularity. This can be done by increasing N or ε^m.

In Table 3 the parameter I_d is varied and, in addition, no upper limit is imposed on N ($N_2 = \infty$). The plasma dimensions and, as a consequence, B_t^o are found to vary only slightly. (Note that B_t^o is determined from the ignition condition.) The coil number increases to 16. The ripple limit is again met. For $I_d > 1$ the horizontal bore for the beam ducts takes its minimum value of 0.7 m. That is, for $I_d > 1$ the limitation of d is more restrictive than condition (1). The full benefit is thus already reached by a 2 N times segmentation.

There is a strong tendency to keep the coil number as low as possible. On the other hand, increased ripple values of up to 1.5 % have been discussed recently /1/. The effect of a variation of ε^m on a system with $I_d = 2$ and N = 12 is therefore shown in Table. 4. Again one finds little impact on the plasma dimensions and B_t^o. The quantity Y is the amount by which R_2 exceeds its minimum as determined by eq. (1) and the condition $d \geq 0.7$ m. If Y > 0 holds, the ripple condition is more restrictive than these two conditions and full benefit of the increased modularity is not taken. To reach Y = 0 requires an ε^m value of 4.5 %. A considerable effect is, however, already achieved by $\varepsilon^m = 1.5$ %, the resulting system being similar to the one with N = 16 and $\varepsilon^m = 0.56$ %. The dependence of E_m and R_2 on ε^m is found to be stronger for low than for high ε^m values.

3.2. Variation of the neutron wall load

If the neutron wall load is reduced, with all other input data kept at their reference values, essentially no effect is observed. The mechanism is quite analogous to the one described above. For a system governed by ALCATOR-like transport scaling there is an intrinsic relation between the neutron wall load N_n, the ignition margin C and the plasma minor radius a:

$$C/N_n \sim a \quad . \qquad (2)$$

From Table 2 it is observed that both C and N_n nearly reach their limit values in the reference system. Hence, anticipating that the minor radius does not vary strongly if N_n is reduced, it follows that N_n and C^m can only be reduced simultaneously.

Table 5 shows a series of runs for various values of N_n^m with C^m reduced to 2. This value of C would roughly correspond to marginal ignition under realistic conditions. It is found that the minor radius indeed increases only slightly when N_n^m is reduced. Accordingly, C decreases with N_n as expected from eq. (2). N_n takes its respective reduced limit value as long as $C > 2$ is valid for the corresponding ignition margin. For N_n^m values below 1 MW/m^2 the limitation on C again becomes effective. Systems with a wall load below 1 MW/m^2 would thus practically require a non-ignited mode of operation. (These statements partly depend on the more optimistic estimate of the fusion power density used here.)

There is a considerable reduction in stored energy which is mainly a consequence of the reduced B_t^o. The size is only slightly reduced, mainly due to the reduction of the coil thickness Δ. Δ decreases since less copper and steel are required for the coil layout if the field is reduced.

3.3 Variation of the neutron fluence

Table 6 shows the impact of a reduction of the minimum neutron fluence W_{int}^m from 6.5 MW y/m^2 to 2.0 MW y/m^2. A reduction of the integral wall load reduces the shielding thickness D. As a result, since the field at the coil is reduced, the coil thickness Δ decreases. Both the reduction of D and Δ reduce the aspect ratio A. The plasma minor radius remains essentiall unchanged.

The effect on E_m and R_2 is rather modest. A drastic reduction of stored energy and size is thus hardly achievable by lowering the fluence objective.

Lowering the neutron fluence might, however, be attractive from a different point of view. Keeping the external tritium supply fixed, reduced tritium consumption would permit reduced blanket coverage. This might considerably ease the access problems especially in the case of higher modularity.

The weak dependence of the size of the system on the integral wall load exhibits a general feature of systems with high absolute $R_o - R_1$. Through the logarithmic dependence of D on W_{int}, D changes only slightly if W_{int} varies in the range under discussion. The impact on the system, on the other hand, depends for a given shift ΔD on the ratio $\Delta D/(R_o - R_1)$. $R_o - R_1$, however, has a relatively high value in systems with superconducting TF coils because of the thermal insulation and the high absolute value of D.

4. Benchmark calculations

Table 7 shows some selected systems within which different parameter variations are combined. They reflect the preceding discussion.

In the first column the reference case is repeated for comparison.

The second column contains representative data for a system with $N_n^m = 1$ MW/m^2 and $W_{int}^m = 1$ MW y/m^2 but the same modularity as the reference system. It visualizes the maximum reduction achievable by reducing only the wall load and fluence.

The system in the third column demonstrates the reduction in size and stored energy that could be achieved by combining an increased modularity with a reduced neutron wall load of 1 MW/m^2. Optimum use is made of the increased modularity by allowing $\varepsilon^m = 1.5$ % and a coil number of 14.

The fourth system is the one closest to the original INTOR performance. It demonstrates the benefit of higher modularity if combined with the relaxed ripple condition and the more optimistic estimate of the fusion power used in SUPERCOIL.

5. Conclusion

The sensitivity of the INTOR layout to variations of the main performance objectives and design specifications is studied with the SUPERCOIL layout model. The stored energy (E_m) and the outer coil radius (R_2) are used as figures of merit. The objectives and specifications under consideration are the neutron wall load, the neutron fluence, the ignition margin and the blanket modularity.

To benefit from a higher blanket modularity, the ripple constraint has to be relaxed by raising the ripple limit or the coil number.

If the ripple limit is fixed to its reference value, a coil number of 16 is required to benefit fully from the increased modularity. If the coil number is kept at its reference value, a ripple of 4.5 % (at boundary) is required to derive full profit from the higher modularity. A considerable effect, however, is already obtained with the recently proposed value of 1.5 %.

An increased modularity is found to be the most effective means of reducing the system, both in size and stored energy. In all cases full benefit is, however, gained from a modularity with is 2 N.

In a system which is governed by ALCATOR-like losses there is an intrinsic coupling between the wall load N_n, the ignition margin C, and the plasma minor radius a in that $C/N_n \sim a$ holds. The minor radius is found to vary only slightly in the present study. Thus, N_n and C can only be reduced simultaneously, a reduction of N_n by roughly 50 % leading to marginal ignition. A reduction of N_n strongly reduces the stored energy of the system but has little effect on the size of the system.

A variation of the neutron fluence in the range 2.0 - 6.5 MW y/m^2 shows a relatively weak impact on the size of the system and stored energy.

References

/1/ Phase II A , European contributions to the 3rd workshop meeting.

Table 1

INPUT

REFERENCE CASE

Constraints

ε^m	(%)	0.56	maximum field ripple (at boundary)
g^m	(m)	0.0	maximum value for g (see Fig. 1)
d^m	(m)	0.7	minimum horizontal bore for beam ports (see Fig. 2)
ΔR^m	(m)	0.0	minimum value for ΔR (see Fig. 1)
N_n^m	(MW/m^2)	1.82	minimum neutron wall load
W_{int}^m	($MW\ Y/m^2$)	6.5	minimum integral wall load
s^m		1.6	maximum plasma elongation
N_1		12	minimum coil number
N_2		12	maximum coil number
C^m		4.0	minimum ignition margin
ε_w^m		1.1×10^{-3}	maximum strain in the winding
σ_{cy}^m	(N/m^2)	3.0×10^8	maximum allowable stress in the support cylinder

Fixed input parameters

δ	(m)	0.15	thermal insulation thickness
ℓ	(m)	0.2	scrape-off layer thickness
u	(m)	0.1	vessel thickness
DB_1	(m)	0.0	blanket thickness at inner side (without shielding)
DB_2	(m)	0.78	blanket thickness at outer side (without shielding)
q (a)		2.1	plasma safety factor
f		1.3	poloidal flux enhancement factor
η_1		0.85	filling factor for the winding
I_{OH}	(A)	2.0×10^4	OH transformer conductor current
V_m	(V)	2.0×10^5	maximum discharge voltage
$\dot{Q}$	(W/m^2)	3.0×10^3	heat flux
T	(K)	4.5	cooling temperature
η_{sc}	(N/m^2)	6.0×10^{11}	Young's modulus of the superconductor
η_{st}	(N/m^2)	1.0×10^{11}	Young's modulus of the stabilizer
η_{re}	(N/m^2)	2.0×10^{11}	Young's modulus of the reinforcing material
η_{cy}	(N/m^2)	2.0×10^{11}	Young's modulus of the central support cylinder
B	(m)	0.05	thickness of coil casing
DF	(m)	5.0×10^{-5}	diameter of the superconducting filament
ΔBV	(T)	0.5	mean amplitude of the perpendicular poloidal magnetic induction at the toroidal winding
ΔBP	(T)	0.5	mean amplitude of the parallel poloidal magnetic induction at the toroidal winding
$\Delta \dot{B}V$	(T/sec)	0.1	magnetic field variation perpendicular to the conductor
$\Delta \dot{B}P$	(T/sec)	0.1	magnetic field variation parallel to the conductor
LP	(m)	0.15	twist length of the conductor

Table 2

OUTPUT

REFERENCE CASE

Geometry

a	(m)	1.18	plasma minor radius
A		4.44	plasma aspect ratio
D	(m)	0.77	shielding thickness
Δ	(m)	0.78	coil thickness
s		1.6	plasma elongation
R_1	(m)	2.45	inner coil radius
R_2	(m)	12.0	outer coil radius
d	(m)	2.69	see Fig. 2

Plasma

N_n	(MW/m^2)	1.84	neutron wall load
W_{int}	($MW\ Y/m^2$)	6.50	neutron fluence
C		4.0	ignition margin (non normalized)
ε	(%)	0.56	field ripple (boundary)
B_t^o	(T)	5.56	field at axis
$\overline{\beta}_t$	(%)	4.33	toroidal beta (volume average, useful part)
P_α	(MW)	165	α-power
I_p	(MA)	6.27	plasma current
V_s	(Vs)	98.7	volt-sec requirement

Toroidal field system

B_m	(T)	10.3	field at coil
Δ_{ax}	(m)	1.49	axial thickness of the TF coil winding
j_{sc}	(A/m^2)	4.3×10^9	current density in the superconductor (TF coil)
$\langle\sigma\rangle$	(N/m^2)	1.73×10^8	average mechanical stress in the winding (TF coil)
E_m	(GJ)	49.7	stored magnetic energy (TF system)
α		121	average ratio of the cross section area between stabilizer and superconductor (TF coil)
β		168	average ratio of the cross section area between reinforcing material and superconductor (TF coil)
$\langle j\rangle$	(A/m^2)	1.26×10^7	average current density in the winding (TF coil)

OH Transformer

t_s	(m)	0.31	thickness of the support cylinder
ϵ_w		1.10×10^{-3}	strain in the winding (TF coil)
R_{OH}	(m)	1.32	OH transformer radius
B_{OH}	(T)	8.95	OH field
ϵ_{OH}		1.09×10^{-3}	OH transformer winding strain

Variation of modularity

$N_1 = 12$
$N_2 = 16$

all other input data see reference case

I_d		1	2	3
a	(m)	1.18	1.12	1.12
A		4.44	4.52	4.52
N		12	16	16
ε	(%)	0.56	0.56	0.56
d	(m)	2.69	0.7	0.7
B_t^o	(T)	5.56	5.74	5.74
E_m	(GJ)	49.6	29.8	29.8
R_2	(m)	12.0	9.7	9.7

Table 4

Variation of ε^m segment. is 2 N times

all other input data see reference case

ε^m	a	A	B_t^o	ε	Y	E_m	R_2
(%)	(m)		(T)	(%)	(m)	(GJ)	(m)
0.56	1.20	4.38	5.49	0.56	3.23	49.1	12.0
0.9	1.18	4.38	5.52	0.9	2.19	39.1	10.9
1.2	1.16	4.38	5.54	1.2	1.67	34.4	10.3
1.5	1.14	4.49	5.70	1.5	1.25	31.8	9.86
3.0	1.19	4.27	5.44	2.9	0.47	24.0	9.05
4.5	1.16	4.31	5.51	4.5	0.0	20.8	8.50

Variation of N_n^m

all other input data see reference case

$C^m = 2$

N_n^m	a	A	Δ	C	E_m	R_2	B_t^o	N_n
(MW/m^2)	(m)		(m)		(GJ)	(m)	(T)	(MW/m^2)
1.82	1.18	4.44	0.78	3.94	48.9	11.9	5.6	1.82
1.5	1.12	4.45	0.72	3.12	41.8	11.5	5.4	1.50
1.0	1.04	4.47	0.63	2.0	30.8	10.8	5.0	1.03
0.5	1.04	4.47	0.63	2.0	30.8	10.8	5.0	1.03

Variation of W_{int}^{m}

all other input data see reference case

$N_1 = 12$

$N_2 = 16$

W_{int}^{m}	a	A	Δ	D	E_m	R_2	N
(MW Y/m^2)	(m)		(m)	(m)	(GJ)	(m)	
6.5	1.18	4.44	0.78	0.77	49.4	12.0	12
5.0	1.19	4.38	0.77	0.75	48.0	11.9	12
3.5	1.19	4.33	0.75	0.72	46.0	11.8	12
2.0	1.19	4.25	0.73	0.69	43.5	11.7	12

Table 7

all other input data
see refernece case

	reference system	$N_n^m = 1$ MW/m^2 $W_{int}^m = 1$ MW Y/m^2 $C^m = 2$	segment is 2 N times $N_n^m = 1$ MW/m^2 $N_1 = 12$, $N_2 = 16$ $\varepsilon^m = 1.5$ % $C^m = 2$	segment is 2 N times $N_n^m = 1.3$ MW/m^2 $\varepsilon^m = 1.5$ % $C^m = 2$
a (m)	1.18	1.07	1.07	1.16
A	4.44	4.25	4.27	4.23
B_t^o (T)	5.56	4.81	4.83	5.02
N	12	12	14	12
Y (m)	0.0	0.0	0.0	1.25
N_n (MW/m^2)	1.82	1.01	1.01	1.30
C	4.00	2.00	2.00	2.75
R_2 (m)	12.0	10.6	8.32	9.54
E_m (GJ)	49.6	27.0	15.5	23.9

Figure 1

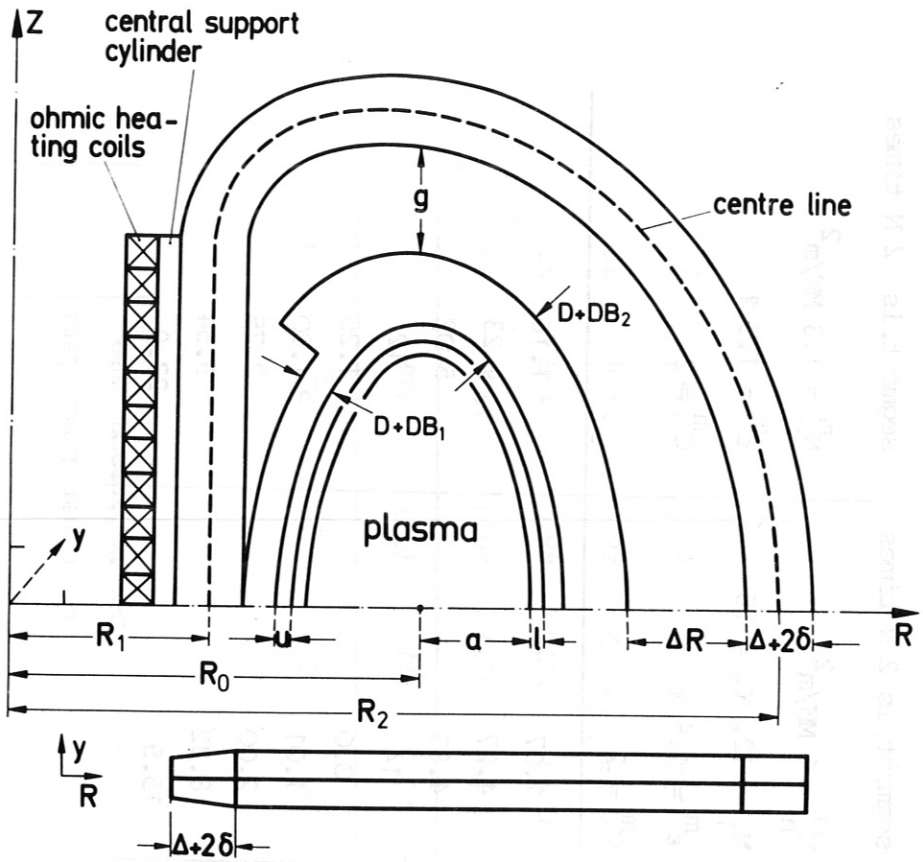

Figure 2